DOI 10.1007/s10553-021-01229-8
Chemistry and Technology of Fuels and Oils, Vol. 57, No.1, March, 2021 (Russian Original No.1, January – February, 2021)

INNOVATIVE TECHNOLOGIES OF OIL AND GAS

EFFECTIVENESS OF COPOLYMER OF POLYMETHYLMETHACRYLATE AND STYRENE AS A PLUGGING AGENT IN WATER-BASED DRILLING FLUIDS

Junwei Fang[1, 2], Yujing Luo[3], Shuanggui Li[1, 2], Mingyi Deng[3], Gang Xie[3*]

In the development of shale gas, it is important to ensure the stability of the borehole wall. The stability of the borehole wall depends on the plugging ability of the drilling fluid, while the stabilizing ability of the drilling fluid is provided by adding the plugging agent to the fluid. Conventional plugging agents are characterized by a relatively high volume and do not allow one to effectively plug micropores and microcracks in shale rock. In this work, the PMMA-St copolymer was synthesized by emulsion polymerization of methyl methacrylate and styrene. The characteristics of the PMMA-St copolymer were studied by FT-IR, TGA, and phase analysis optical scanning methods. The results show that the size of PMMA-St nanoparticles ranges from 34 to 58 nm, and the average diameter is about 40.6 nm. The decomposition temperature of PMMA-St nanoparticles is 374.8°C, which indicates the good thermal stability of the copolymer. The PMMA-St nanoparticles have little effect on the rheological properties of water-based drilling fluids. The mud cake simulation method was used to evaluate the plugging performance of PMMA-St nanoparticles. The permeability of mud cake is 2.24×10^{-5} m^2, which is close to the permeability of shale formation. When 0.5 wt % of

[1]Petroleum Engineering Technology Research Institute, Northwest Oilfield Company, Sinopec, Urumqi, Xinjiang, 830011, China. [2]Key Laboratory of Enhanced Recovery for Fracture-Cave Oil Reservoir, Sinopec, Urumqi, Xinjiang, 830011, China. [3]State Key Laboratory of Oil and Gas Reservoir Geology and Exploitation of Southwest Petroleum University, Chengdu, 610500, China.*Corresponding author:Gang Xie. E-mail: 201899010129@swpu.edu.cn..* Translated from *Khimiya i Tekhnologiya Topliv i Masel*, No. 1, pp. 57-61, January – February, 2021.

the PMMA-St copolymer is added to the solution, the blocking rate is 70.27%. With increase in PMMA-St concentration, the blocking rate of the mud cake increases. The best stabilizing effect is achieved when the PMMA-St copolymer concentration is 1.0%. The results of the core experiments are consistent with the mud cake simulation, which indicates the excellent sealing ability of the PMMA-St copolymer. Therefore, PMMA-St nanoparticles can be effectively used as a plugging agent to ensure borehole stability in the shale formation.
Keywords: *nanoplugging agent; PMMA-St copolymer; mud cake; plugging performance.*

1 INTRODUCTION

Shale gas is a relatively clean, low-pollution, and low-cost unconventional natural gas resource, which has been recently widely developed worldwide [1]. The potential of shale gas resources is high, and the exploration and development of shale gas have become a research hotspot. From the perspective of conventional shale gas exploration and development methods, shale gas formation is low in strength, brittle, and prone to instability and collapse. The mud shale is very susceptible to hydration and dispersion, which seriously restricts shale gas production. To prevent hydration, oil-based drilling fluids are commonly used in shale gas production [2 - 4]. Oil-based drilling fluids provide good wellbore stability and shale suppression performance. However, due to hydraulic fracturing, oil-based drilling fluids can cause wall instability and severe environmental pollution. Therefore, the use of oil-based drilling fluids is restricted by environmental protection regulations [5]. The formation instability is the main reason for the borehole wall collapse. Mud shale formation is characterized by numerous microporous fractures. The pore size of microfractures in mud shale is extremely small [6 - 8]. Therefore, the particle size of the plugging agent material in the drilling fluid must meet strict requirements [9]. In a conventional plugging agent, the particles are not prone to squeezing and deforming, which prevents them from entering the microcracks in shale [10]. On the other hand, the advantages of the plugging nanomaterials include small particle size, elasticity to deformation, size adjustability, and large surface area [11]. Adding nanoparticles to the drilling fluid can effectively seal microfractures and prevent water from entering the shale. Therefore, the preparation of a nano-size plugging material compatible with water-based drilling fluids has important practical significance [12].

The particle size of most commonly used plugging agents such as fine calcium carbonate, asphalt, and walnut shell powder is larger than the size of nanopores in the shale formation. The size of pores in the shale formation ranges from 1 to 100 nm. Conventional plugging agents do not provide effective sealing when drilling in the shale formation. To provide sealing, it is important to develop a sealing agent containing nano-size particles [14,15]. Some recently developed plugging agents, including nanosilica, nanographene, cellulose nanoparticles, carbon nanotubes, hyperbranched polymers, and other materials, have been widely used in drilling fluids [16]. Due to the nano-scale effect, the nanomaterial is prone to agglomeration, making it difficult to maintain the nano-scale size of particles in the solution. Most inorganic nanoparticles cannot maintain suspension stability in the drilling fluid system for a long time. The polymer nanoparticles can remain stable in the emulsion for a long time [18,19].

In this work, we have developed a new polymer material to be used as a plugging agent. The PMMA-St copolymer was prepared by emulsion polymerization using methyl methacrylate and styrene as raw materials. The properties of the PMMA-St copolymer were studied by Fourier transform infrared spectroscopy (FT-IR), particle size analysis, thermogravimetric analysis, and scanning electron microscopy (SEM). The plugging performance of the anion core-shell copolymer was studied by core simulation tests.

2 MATERIALS AND METHODS

2.1 MATERIALS

Methyl methacrylate, styrene, potassium sulfate, potassium peroxymonosulfate, and sodium lauryl sulfate were purchased from J&K Scientific Ltd. Bentonite was from Xinjiang Xiazijie. Industrial grade sulfonated lignite, sulfonated phenol-formaldehyde resin, carboxymethyl cellulose sodium, lignite sodium humate, and barite were obtained from a commercial corporation.

2.2 METHODS

Fourier transform infrared spectrometer (FTIR, Nicolet 6700, Thermo Scientific) was used to characterize the copolymer. The particle size analysis of the core-shell copolymer was performed in the Brookhaven ZetaPALS laboratory. The microstructure of the core-shell copolymer was studied by scanning electron microscopy (Quanta 450, FEI, USA). Thermogravimetric analysis (TGA/DSC1, Mettler, Switzerland) was used to measure the thermal stability at a temperature rise rate of 15!/min in the range from 30 to 300°C. The rheological properties of water-based drilling fluids were measured using a ZNND6 rotational viscometer developed by Qingdao Jiaonan Tongchun Machinery Petroleum Instrument Ltd., China.

2.3 FLUID PREPARATION AND THERMAL AGING TESTS

The drilling fluid formula is 100 g water + 5% Na + Mt + 0.5% Na_2CO_3 + 0.8% sodium carboxymethylcellulose + 3% lignite sodium humate + 10% barite. The content of Na + Mt, sodium carboxymethylcellulose, sodium humin, and barite is determined by the water content. The obtained drilling fluid was used to evaluate the rheological properties of the inhibitors.

2.4 RHEOLOGICAL PARAMETERS EVALUATION

The rheological parameters such as apparent viscosity (AV), plastic viscosity (PV), and yield point (YP) were calculated from the rheometer readings in the range from 600 to 300 rpm using the following formulas [20]:

$$\text{Apparent viscosity (AV)} = Ø\ 600/2\ (\text{mPa·s}), \tag{1}$$

$$\text{Plastic viscosity (PV)} = Ø\ 600 - Ø\ 300\ (\text{mPa·s}), \tag{2}$$

$$\text{Yield point (YP)} = (Ø\ 300 - \text{PV})/2\ (\text{Pa}). \tag{3}$$

2.5 PLUGGING EVALUATION METHOD

2.5.1 Preparation of mud cake

First, 10 g of bentonite and 0.5 g of sodium carbonate were slowly added to 100 mL of boiling water and the whole stirred vigorously for 4 h. Then 5 g of sulfonated lignite was added to the solution and the mixture stirred for 1 h. Then 5 g of the sulfonated phenol resin was added and the mixture stirred vigorously for 1 h. Finally, 100 g of barite was added and the whole vigorously stirred for 1 h. The mixture was left to cure for 24 h.

Before measuring the filtration volume, the resulting standard mud was stirred vigorously for 0.5 h and then placed in the HTHP filter device. The filtration volume was measured at 105°C and 3.5 MPa for 30 min, and the initial and final filtration volumes were recorded. The fluid was poured out, and the mud cake was washed

with distilled water. The distilled water was slowly injected into the HTHP filter press along the inner wall, and the filtration volume of the distilled water was measured at 105°C and 3.5 MPa. Data were recorded for 30 min with a 5-min step. The mud cake was then used for the evaluation of the plugging performance of the nanomaterial.

2.5.2 Evaluation of mud cake

The mud cake permeability was evaluated using the drilling fluid filtrate. To evaluate the plugging performance of the PMMA-St material, the PMMA-St nanoparticles were added to the filtrate. The permeability of the mud cake was calculated as

$$K = \frac{h\mu Q_t}{A\Delta P} \tag{4}$$

where K is the permeability of mud cake, 10^{-5} μm^2; A is the cross-sectional area of mud cake, cm^2; ΔP is the differential pressure, MPa; h is the mud cake thickness, cm; μ is the viscosity of the solution containing PMMA-St nanoparticles, mPa·s; and Q_t is the average flow rate, $cm^3 \cdot s^{-1}$.

The plugging rate of mud cake was calculated as [11]

$$W = \frac{(K_1 - K_2)}{K_1} \times 100\% \tag{5}$$

where W is the plugging rate; K_1 is the mud cake permeability to water without PMMA-St nanoparticles, and K_2 is the mud cake permeability to the solution containing different concentrations of the PMMA-St nanoparticles.

2.6 SYNTHESIS OF PMMA-ST COPOLYMER

The measured amount of sodium styryl sulfonate, accounting for 70% of the total monomers, a small amount of potassium sulfate, and a small amount of sodium dodecyl sulfate are placed in a 1-liter three-neck flask in nitrogen atmosphere, and 400 g of deionized water is added to dissolve the mixture; then methyl methacrylate (30 g) and styrene dissolved in nitrogen (30g) are added to the mixture, and the mixture is stirred at 300 rpm and 67°C. To initiate polymerization, a 20 g solution containing 0.45 g potassium persulfate is added

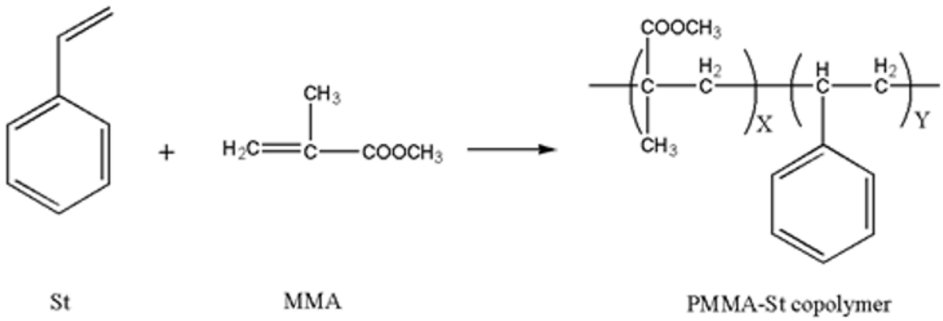

Fig.1. Copolymerization reaction of methyl methacrylate and styrene.

to the mixture. The reaction takes 24 h. The reaction of copolymerization of methyl methacrylate and styrene is shown in Fig.1.

3 RESULTS AND DISCUSSION

3.1 FT-IR

The FT-IR spectrum of the PMMA-St copolymer is shown in Fig. 2. As shown in Fig. 2, the peak at 3462 cm^{-1} is the stretching vibration peak of –OH bond formed by residual water and sodium sulfonate group. The peak at 1735 cm^{-1} is attributed to the C=O bond, and the peak at 1182 cm^{-1} to the C-O bond. Both peaks are characteristic of the ester group (-$COOCH_3$). The peak at 2925 cm^{-1} is due to the extension of -CH_2 and -CH_3 bonds. The peaks at 1603, 1590, and 1500 cm^{-1} are the skeletal vibration peaks of the benzene ring. The peaks at 758 and 702 cm^{-1} are the vibrational characteristic absorption peaks of the monosubstituted benzene ring [13]. The results show that the synthesized copolymer contains the ester group, benzene ring, methyl group, and methylene group, indicating that the PMMA-ST copolymer is successfully synthesized and the structure ideally corresponds to the designed structure.

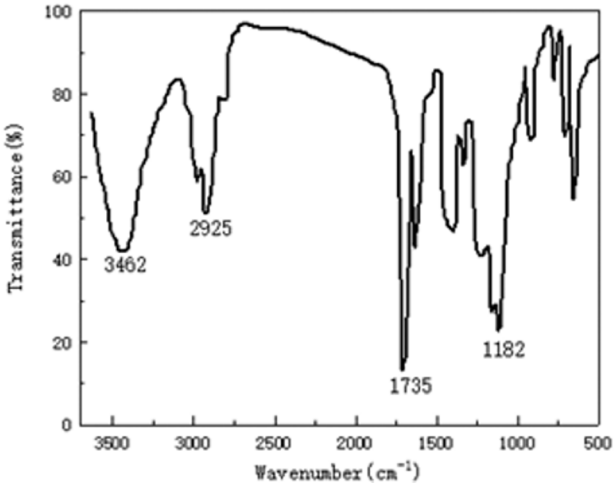

Fig.2. FT-IR spectrum of PMMA-St copolymer.

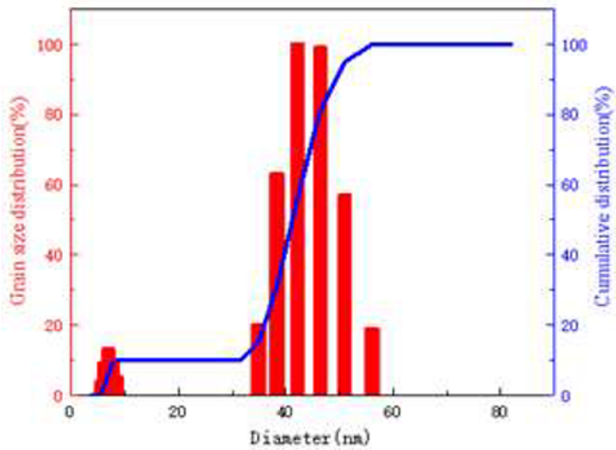

Fig.3. The grain size distribution and cumulative distribution of the PMMA-St copolymer nanoparticles.

3.2 GRAIN SIZE DISTRIBUTION

The size of the PMMA-St copolymer particles was measured using a Brookhaven laser particle size analyzer ZetaPALS. Figure 3 shows that the particle size distribution of the PMMA-St copolymer is relatively narrow. Most of the grain size is distributed in the range of 34-58 nm, with a small distribution peak at 5-10 nm. The average grain diameter is 40.6 nm. This shows that PMMA-St nanoparticles of size smaller than 100 nm can effectively block nano-scale pores and fractures in shale. Therefore, PMMA-St nanoparticles can be effectively used in water-based drilling fluids.

3.3 THERMOSTABILITY OF PMMA-ST NANOPARTICLES

The thermogravimetric curve of the PMMA-St nanoparticles is shown in Fig. 4. As shown in Fig. 4, the initial decomposition temperature of the copolymer is 374.8°C, which indicates that the PMMA-St nanoparticles

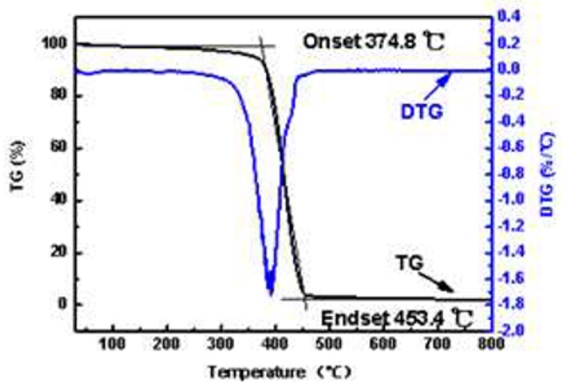

Fig.4. Thermogravimetric analysis of PMMA-St nanoparticles.

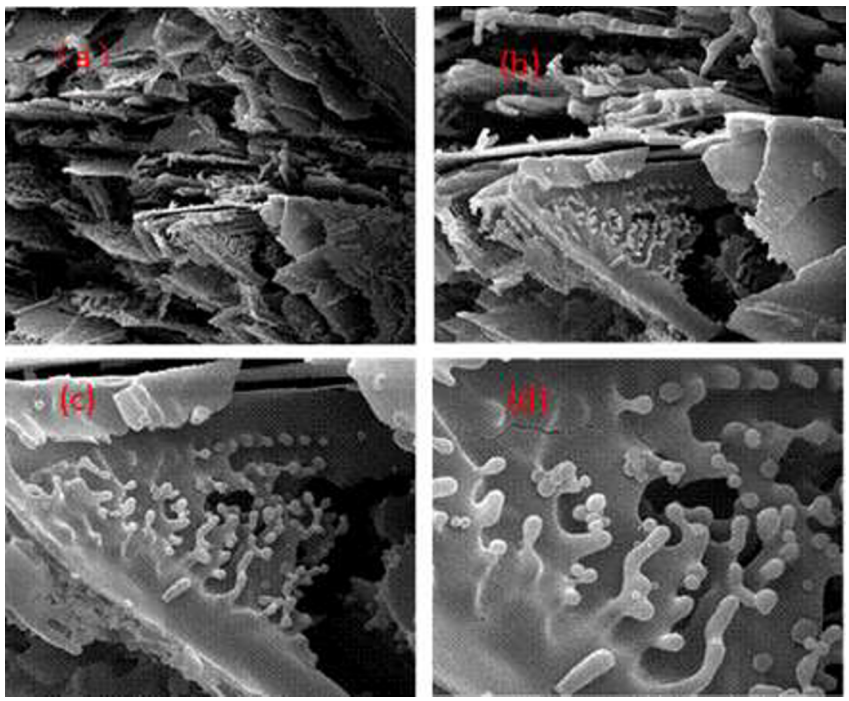

Fig. 5. SEM images of the PMMA-St nanoparticles at different magnification. a) 1000×, b) 2000×, c) 5000×, and d) 10000×.

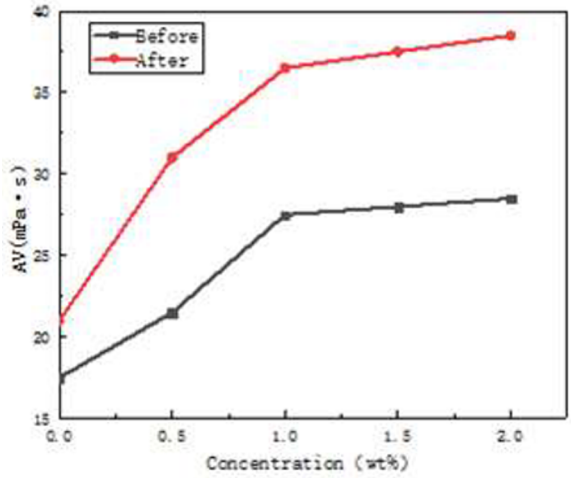

Fig. 6. AV data of drilling fluids with different PMMA-St nanoparticle concentrations (before and after hot rolling tests at 105°C for 16 h).

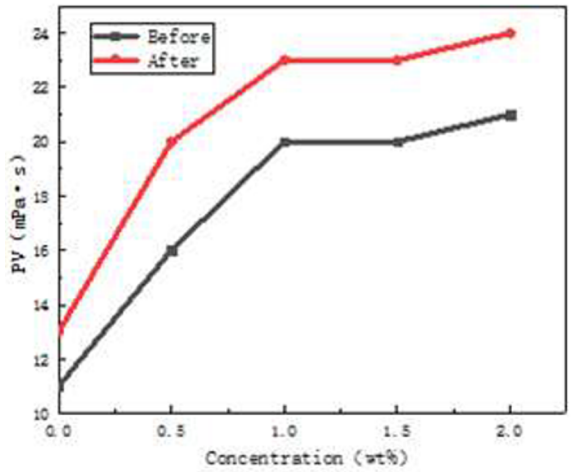

Fig. 7. PV data of drilling fluids with different PMMA-St nanoparticle concentrations (before and after hot rolling tests at 105°C for 16 h).

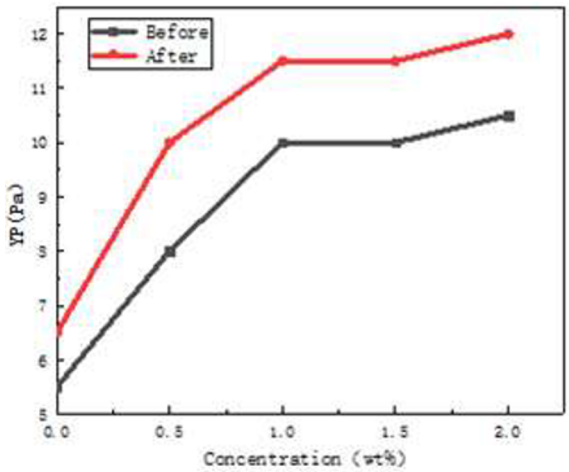

Fig. 8. YP data of drilling fluids with different PMMA-St nanoparticle concentrations (before and after hot rolling tests at 105°C for 16 h).

remain stable when the temperature is lower than 374.8°C. With further increase in temperature, the PMMA-St nanoparticles begin to decompose due to the decomposition of the polymer. When the temperature rises from 374.8°C to 453.4°C, the weight of the PMMA-St nanoparticles decreases by 90.56%. The results show that the PMMA-St nanoparticles have good temperature resistance and can be used in high-temperature deep-well drilling processes.

3.4 SEM

Figure 5 shows the SEM images of the PMMA-St nanoparticles at different magnifications. The results show that the PMMA-St copolymer consists of multiple sheet-like structures. However, the particle size results indicate that the PMMA-St nanoparticles are spherical in shape. The reason is that the SEM image shows the original structure of the PMMA-St nanoparticles, while the particle size analysis measures the dynamic particle size of the PMMA-St particles containing the hydrated shell of the PMMA-St copolymer. The SEM image of the PMMA-St copolymer proves the dense structure of the particles.

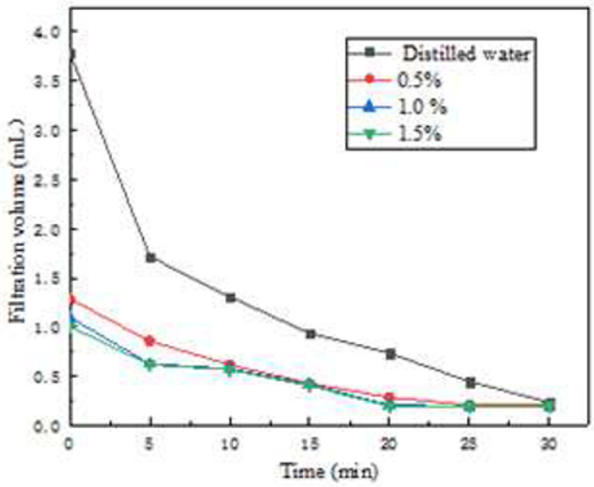

Fig. 9. The filtration volume of mud cake with different concentrations of PMMA-St nanoparticles at different times.

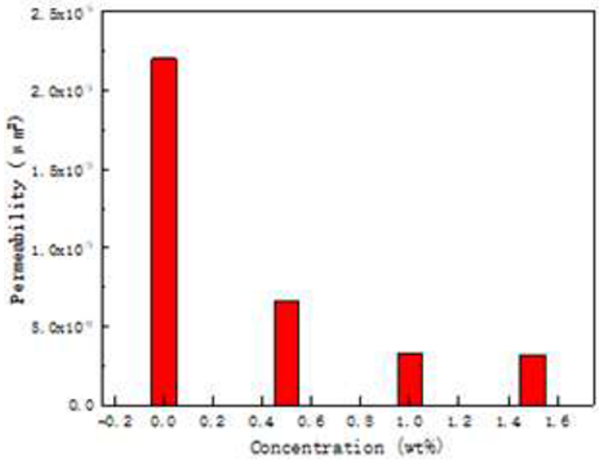

Fig.10. The permeability of mud cake with different concentrations of PMMA-St nanoparticles.

3.5 RHEOLOGICAL AND FILTRATE PROPERTIES OF WATER-BASED DRILLING FLUID

To study the rheological behavior of the drilling fluids, different concentrations of the PMMA-St nanoparticles (0, 0.5, 1, 1.5, and 2%) are added to the basic drilling fluid. The rheological properties (AV, PV, and YP) of the fluids are shown in Figs. 6, 7, and 8, respectively. The results show that when the nanoparticles are added to the solution, the rheological parameters (AV, PV, YP) of the fluids increase both before and after hot rolling treatment at 105°C for 16 h. The reason for the increase at 105°C is that when the PMMA-St nanoparticles are added to the drilling fluid system, they cause an increase in the structural viscosity of the drilling fluid. However, when the concentration of nanoparticles exceeds 1%, the rheological parameters before and after the hot rolling test increase insignificantly. This shows that the viscosity of the PMMA-St copolymer is very low and has little effect on the rheological properties of water-based drilling fluids. The results show that the optimal amount of the PMMA-St nanoparticles is 1.0 %.

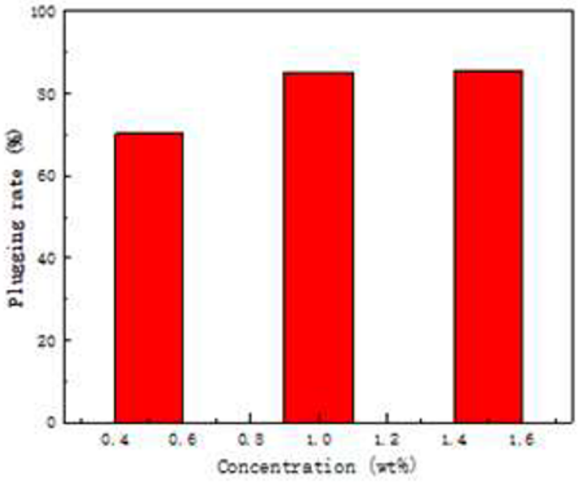

Fig.11. The plugging rate of PMMA-St nanoparticles of different concentrations.

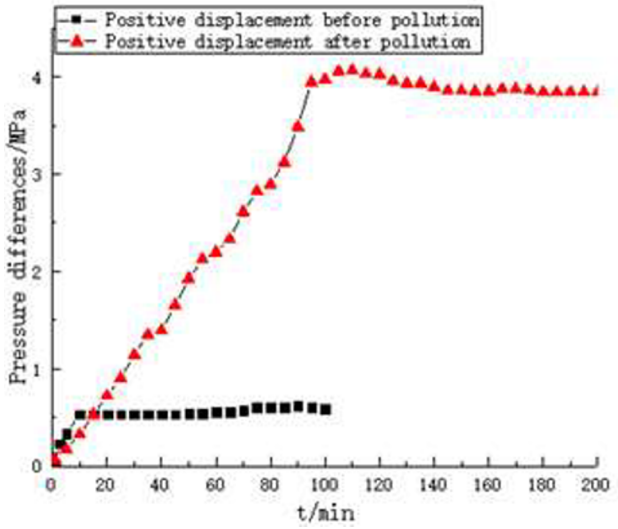

Fig.12. The displacement pressure curves of artificial core water-based drilling fluid without PMMA-St.

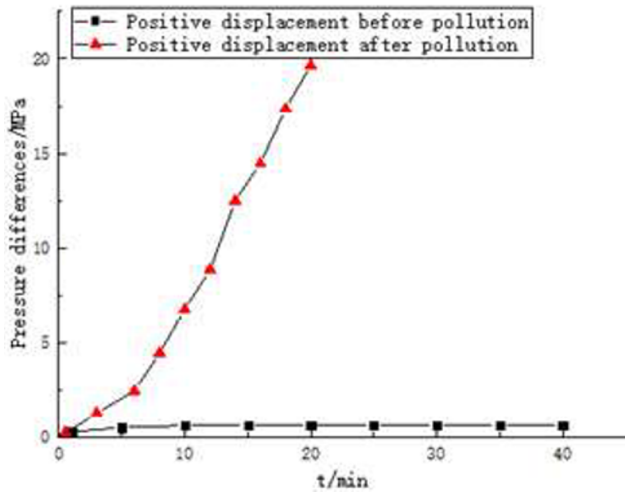

Fig.13. The displacement pressure curves of artificial core water-based drilling fluid containing 1% PMMA-St.

3.6 PLUGGING PERFORMANCE OF PMMA-ST NANOPARTICLES

3.6.1 Evaluation of mud cake

To simulate the formation core, mud cake evaluation tests were carried out. The mud cake tests have the advantages of low cost and good reproducibility. The filtration volume of the PMMA-St copolymer nanoparticles with different concentrations at different times is shown in Fig. 9. The results show that compared with the filtration loss volume of the mud cake containing filtrate, the filtration loss volume of the mud cake containing the PMMA-St nanoparticles is significantly reduced. As the PMMA-St concentration increases, the filtration volume decreases. The permeability of the mud cake calculated from Eq. (4) is $2.24 \times 10^{-5} \mu m^2$, which is close to the permeability of shale, as shown in Fig. 10. The results show that the mud cake tests can succefully simulate the plugging performance of the PMMA-St copolymer nanoparticles. The permeability of the mud cake decreases with increase in the PMMA-St nanoparticle concentration. As shown in Fig. 11, when the PMMA-St concentration is 0.5 %, the blocking rate calculated from Eq. (5) is 70.27 %. When the PMMA-St concentration is 1.0% and 1.5%, the mud cake plugging rate is 85.13% and 85.58%, respectively. The plugging rate of the mud cake increases with increase in the PMMA-St nanoparticle content amount. When the concentration exceeds 1.0%, the plugging rate changes insignificantly. The results show that the optimal concentration of the PMMA-St nanoparticles providing a good blocking performance is 1.0%.

3.6.2 Evaluation of artificial core

The displacement pressure curves obtained by the core evaluation tests are shown in Figs.12 and 13. Figure 12 shows the displacement pressure curves of the water-based drilling fluid without PMMA-St. The positive displacement pressure peak is only 0.61 MPa before the core contamination with the water-based drilling fluid without PMMA-St. After contamination, the positive displacement pressure peak is about 4.06 MPa for a test time of 110 min. Figure 13 shows the displacement pressure curves of the water-based drilling fluid containing 1.0% of PMMA-St. As can be seen from the figure, the peak of positive displacement pressure is as low as 0.63 MPa. When the water-based drilling fluid contains 1.0% of PMMA-St, the positive displacement pressure peak is 19.65 MPa. The permeability of the core to the water-based drilling fluid containing 1.0 % PMMA-St is $3.3 \times 10^{-6} \mu m^2$, as calculated from Eq. (4). This is consistent with the results obtained from the mud cake evaluation. The results prove that the core permeability can be measured by either of these two methods and that the PMMA-St copolymer demonstrates good

plugging performance. The length of the articial core is 5.45 cm, the cross-sectional diameter is 2.44 cm, and the porosity is 4.79%.

4 CONCLUSIONS

PMMA-St copolymer nanoparticles were prepared by emulsion polymerization of styrene and MMA monomers. The PMMA-St material was characterized by FT-IR, TGA, and phase analysis by the light adsorption method. The size of the PMMA-St nanoparticles ranges from 34 to 58 *n*m, and the average diameter is about 40.6 *n*m. The PMMA-St nanoparticles are smaller than 100 nm and can effectively block pores and cracks in the shale formation. The PMMA-St nanoparticles have good temperature resistance, and the polymer decomposition temperature is higher than 374.8!.

The shale formation parameters are simulated by a low-permeability mud cake method. When the water-based drilling fluid contains the PMMA-St nanoparticles, the permeability of the mud cake decreases sharply with increase in the PMMA-St concentration. When the PMMA-St nanoparticles concentration exceeds 1.0 %, the blocking effect is good. The results of the core evaluation are consistent with the mud cake simulation experiment, which shows that the PMMA-St material provides an excellent sealing effect. Therefore, PMMA-St nanoparticles can be used as an effective nano-blocking agent to provide borehole wall stability in shale.

CONFLICT OF INTERESTS

The authors declare no conflict of interests.

ACKNOWLEDGMENT

This work was financially supported by the Major Science and Technology Project of China Petrochemical Co., Ltd., "Shunbei Oil and Gas Field Fast Drilling Technology Research "(P18021-2).

REFERENCES

1. M. Melikoglu, "Shale gas: Analysis of its role in the global energy market," *Renew. Sustain. Energ. Rev.*, 37, 460-468 (2014).
2. C. McGlade, J. Speirs, and S. Sorrell, "Unconventional gas - a review of regional and global resource estimates," *Energy*, 55, 571-584 (2013).
3. X. Wang and R. Sterling, "Stability analysis of a borehole wall during horizontal directional drilling," *Tunnel. Undergr. Space Technol.*, 22, 620-632 (2007).
4. G. Bol, S. W. Wong, C. Davidson, and D. Woodland, "Borehole stability in shales," *SPE Drill. Compl.*, 9, 87-94 (1994).
5. T. J. Srivatsa and M. B. Ziaja, "An experimental investigation on use of nanoparticles as fluid loss additives in a surfactant-polymer based drilling fluids," Conference proceedings, *SPE – IPTC*, 3, 280-00226 (2012).
6. J. Cai, M. E. Chenevert, M. M. Sharma, and J. E. Friedheim, "Decreasing water invasion into Atoka shale using nonmodified silica nanoparticles," *SPE Drill. Complet.*, 27, 103-112 (2012).
7. C. Temple and A. Youngson, "Drilling fluids with improved shale inhibition and methods of drilling in subterranean formations," Patent US7786049B2 (2006).
8. T. Zhang, D. Davidson, and S. Bryant, "Nanoparticle-stabilized emulsions for applications in enhanced oil recovery," *SPR Improved Oil Recovery Symposium*, Tulsa, Oklahoma, USA (2010).

9. M. C. Li, Q. Wu, K. Song, Y. Qing, and Y. Wu, "Cellulose nanoparticles as modifiers for rheology and fluid loss in bentonite water-based fluids," *ACS Appl. Mater. Interfaces*, 7, 5006-5016 (2015).
10. L. Ma, Y. He, P. Luo, L. Zhang, and Y. Yu, "Automatic dispersion, long-term stability of multi-walled carbon nanotubes in high concentration electrolytes," *J. Nanopart. Res*., 20(2), 45-57 (2018).
11. G. Xie, P. Luo, M. Deng, Z. Wang, and R. Gong, "Hyperbranched polyamine as nano-plugging agent used in water-based drilling fluid," *Nanosci. Nanotechnol. Lett*., 9, 310-315 (2017).
12. Y. An, G. Jiang, Y. Ren, L. Zhang, Y. Qi, and Q. Ge, "An environmental friendly and biodegradable shale inhibitor based on chitosan quaternary ammonium salt," *J. Pet. Sci. Eng*., 135, 253-260 (2015).
13. H. Xianbin, S. Haokun, and S. Jinsheng, "Nano laponite as a potential shale inhibitor in water based drilling fluid for stabilizing wellbore stability and mechanism study," *ACS Appl. Mater. Interfaces*, 10(39), 419-427 (2018).
14. M. M. Barry, Y. Jung, and J. K. Lee, "Fluid filtration and rheological properties of nanoparticle additive and intercalated clay hybrid bentonite drilling fluids," *J. Pet. Sci. Eng*., 127, 338-346 (2015).
15. D. Lin-Vien, N. B. Colthup, W. G. Fateley, and J. G. Grasselli, *The Handbook of Infrared and Raman Characteristic Frequencies of Organic Molecules*, Academic Press, New York (1991).
16. L. Xiongli, W. Yangbing, J. Qu, et al., "Improving salt tolerance and thermal stability of cellulose nanofibrils by grafting modification," *Carbohydr. Polym*., 211, 257-265 (2019).
17. S. Paikaray, S. Banerjee, and S. Mukherji, "Surface characteristics of shales and implication on metal sorption," *Environ. Chem. Lett*., 6, 91-94 (2008).
18. M. K. Rahman, D. Naseby, and S. S. Rahman, "Borehole collapse analysis incorporating time-dependent pore pressure due to mud penetration in shales," *J. Pet. Sci. Eng*., 28, 13-31 (2000).
19. M. Khodja, J. P. Canselier, F. Bergaya, K. Fourar, M. Khodja, N. Cohaut, and A. Benmounah, "Shale problems and water-based drilling fluid optimisation in the Hassi Messaoud Algerian oil field," *Appl. Clay Sci*., 49(4), 383-393 (2010).
20. A. Yuxiu, J. Guancheng, and Q. Yourong, "High-performance shale plugging agent based on chemically modified graphene," *J. Nat. Gas Sci. Eng*., 32, 347-355 (2016).